

FIG. 3. Time dependence of arc current (1, 4) and voltage on the arc (2, 3): 1, 2) theory; 3, 4) experiment.

$$(I/I^*)^2 + \lambda(t/\tau_L)^2 = 1, \quad (10)$$

where  $\lambda = \nu\tau_L \tan \alpha / L_{\text{noneq}}$  is a small parameter, numerically equal to 0.03. It is seen that the influence of inductance prolongs the life of the discharge by about  $\tau_L/\sqrt{\lambda} \sim 5$  msec, which corresponds to an increase in power in the extinction process by  $\sqrt{\lambda} \approx 20\%$ . In Fig. 3 we give numerical solutions of Eq. (2) for the time dependence of the current and voltage in the arc, and it is seen that they agree fairly well with the experimental functions also given there.

A sliding arc thus consists of a discharge system at atmospheric pressure in which, at a high power level, one can

continuously (although not steadily) maintain highly nonequilibrium conditions, of interest for plasma-chemical applications, in particular. In its physical parameters, a sliding arc is closer than other types of discharges to a nonequilibrium UHF discharge at medium pressure, which suggests a high efficiency for carrying out in it such endoergic reactions as  $\text{CO}_2$  dissociation, water decomposition, the conversion of methane into acetylene, etc.<sup>1</sup> A sliding arc may also be efficient in gas purification, since the energy cost per active particle is several times lower here than in a barrier, corona, or beam discharge. A drawback of a sliding arc for air purification is the possibility of the simultaneous production in the hot equilibrium regions of harmful substances, primarily nitric oxides. A sliding arc actually is a less selective but simultaneously more powerful means of purification.

<sup>1</sup>V. D. Rusanov and A. A. Fridman, *Physics of a Chemically Active Plasma* [in Russian], Nauka, Moscow (1980).

<sup>2</sup>Yu. P. Raizer, *Physics of a Gas Discharge* [in Russian], Nauka, Moscow (1987).

<sup>3</sup>H. Lesuer, A. Czernichowski, and J. Chapelle, *Demande Brevet Francais* **88**, 1492 (1989).

<sup>4</sup>H. Lesuer, A. Czernichowski, and J. Chapelle, *Colloque Phys. Colloque C5*, Suppl. 18, 51 (1990).

<sup>5</sup>V. V. Liventsov, B. V. Potapkin, V. K. Roddatis, et al., *Teplofiz. Vys. Temp.* **27**, 220 (1989).

<sup>6</sup>A. S. Petrushev, B. V. Potapkin, V. D. Rusanov, and A. A. Fridman, *Teplofiz. Vys. Temp.* **28**, 1072 (1990).

Translated by Edward U. Oldham

## Structural changes in tsaregorodtsevite

E. V. Sokolova, V. B. Rybakov, L. A. Pautov, and D. Yu. Pushcharovskii

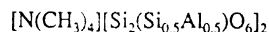
*M. V. Lomonosov State University, Moscow*

(Presented by Academician V. A. Zharikov, March 16, 1993)

(Submitted March 16, 1993)

Dokl. Akad. Nauk **332**, 309–311 (September 1993)

Among known minerals containing organic cations, tsaregorodtsevite



stands out due to the presence of the tetramethylammonium cation (TMA). Before this mineral was discovered and its structure deciphered,<sup>2</sup> silicates with the polyatomic TMA cation were considered as extremely unstable compounds (rapidly decomposing in air) in which the interaction between the cationic and anionic parts is markedly weak.<sup>3</sup> In contrast to the overwhelming majority of silicates, the (Si, O) complexes detected when the structure of synthetic TMA silicates was deciphered are rather unusual paired quadrupole and triple rings, which according to Ref. 4 form the basis of these structures. Support for this conclusion comes from the relative arrangement of the cations and anions, in which the nuclei of the complex cations are located on opposite faces of the silicate anion, surrounding it with the cationic polyhedron formed.

Thus this group of silicates, along with zeolites,<sup>4</sup> has been recently considered as a definite exception to the N. V. Belov principle of the adaptability of (Si, O) complexes to the cationic structure. The presence of the TMA cation along with alkali cations (Na, Li) has also been noted in a number of zeolites, and some of them (offretite and EAB) are obtained from solutions in which the presence of the  $\text{Na}^+$  cation is necessary in addition to TMA.<sup>6</sup>

A structural study of tsaregorodtsevite has allowed us to establish its similarity to sodalite. When the symmetry of the tetrahedral framework decreases from cubic in sodalite to rhombic in tsaregorodtsevite, a major macroscopic difference between the two structures involves the location of TMA cations in the clathrosil cavities of tsaregorodtsevite instead of  $\text{Cl}^-$  anions in sodalite and a somewhat different rotation of the tetrahedra relative to each other. The DTA investigation of tsaregorodtsevite (undertaken after the structure was deciphered) detected weight loss in its calcination products at temperatures from 660°C to 950°C. When annealing the min-

eral in a stream of purified helium, the ammonia evolved upon heating was determined. In this case, the gaseous products were absorbed by a solution of hydrochloric acid, and the determination of ammonia was completed either titrimetrically or calorimetrically with Nessler's reagent. With some spread in the results, the mass of the evolved  $\text{NH}_3$  was estimated as 1.3-1.6 mass%. Evolution of another water-soluble gas was detected during calcination which could not be identified. Certain changes in the composition and properties of tsaregorodtsevite at high temperatures stimulated a structural study of the products of its annealing at 870 and 970°C. The experimental characteristics determined by deciphering the structure of the annealed crystals (using the single-crystal CAD-4 diffractometer for phase I and the Syntex PI diffractometer for phase II, and the SDP and INEXTL program packages respectively) are presented in Table I. The coordinates of the basis atoms, the equivalent temperature factors, the interatomic distances, and the bond angles in the structures of tsaregorodtsevite and its annealing products are presented in Tables II and III. For convenience in comparing the atomic coordinates (Table II) in the structures of phases I, II, and tsaregorodtsevite, in the latter we interchanged the locations of the  $x$  and  $z$  axes.

With an increase in temperature, the symmetry of the Si-Al-O framework increases from rhombic (space group  $I222$ ) to cubic (space group  $I432$ ); in this case, the axial symmetry of the unit cell is preserved and its volume decreases. The increase in symmetry is connected with redistribution of the Si and Al cations in the framework: in tsaregorodtsevite, the Si atoms are distributed over two four-fold positions  $4(h)$  ( $1/2 y 0$ ) and  $4(j)$  ( $0 1/2 z$ ), where  $y \approx z \approx 0.75$ ; and in the tetragonal modification, the Si atoms occupy one eight-fold position  $8(i)$  ( $x 0 1/2$ ), where  $x \approx 0.25$ , which leads to a four-fold axis arising along the  $a$  axis (different from the other two, Table I) of the rhombic unit cell of tsaregorodtsevite. The two independent O atoms also merge into one eight-fold position  $8(g)$  ( $x x 0$ ). Upon calcination up to 870°C, the mineral loses  $\approx 9\%$  of its weight and takes on a black color. These phenomena are probably connected with breakdown of the complex cations  $[\text{N}(\text{CH}_3)_4]^+$  in the tsaregorodtsevite structure. In the channels of the mineral structure, we detect maxima in the

TABLE II. Coordinates and Isotropic Equivalent Temperature Factors ( $\text{\AA}^2$ ) for Basis Atoms in Structures of Tsaregorodtsevite and Its Annealing Products

Atom	$x/a$	$y/b$	$z/c$	$B_{\text{equ}}$
Tsaregorodtsevite				
Si1	0.5	0.2511(2)	0	1.08(2)
Si2	0.2491(2)	0	0.5	1.05(2)
( $\text{Si}_{0.5}\text{Al}_{0.5}$ )	0	0.5	0.2498(1)	1.09(2)
O1	0.003(3)	0.3550(5)	0.3537(4)	3.45(9)
O2	0.3509(6)	-0.001(2)	0.3544(4)	3.8(1)
O3	0.3531(6)	0.3540(6)	0.007(2)	3.9(1)
N	0	0	0	1.8(1)
C1*	0.001(1)	0.127(3)	0.116(3)	3.8(5)
C2*	0.126(3)	0.007(1)	0.119(3)	4.8(5)
C3*	0.121(4)	0.117(4)	0.001(1)	4.9(6)
Phase I				
Si	0.2489(1)	0	0.5	1.95(2)
( $\text{Si}_{0.5}\text{Al}_{0.5}$ )	0	0.5	0.25	2.02(2)
O1	0.3539(3)	0.3539(3)	0	5.5(1)
O2	0.3503(3)	-0.010(1)	0.3538(4)	4.89(7)
C**	0.070(2)	0.105(2)	0.088(2)	4.3(3)
Phase II				
( $\text{Si}_{0.833}\text{Al}_{0.167}$ )	0.25	0.5	0	4.4(1)
O	0	0.3558(7)	0.3558(7)	7.8(4)

Note. A single asterisk indicates C atoms statistically occupying 1/3 of their position; a double asterisk indicates C atoms statistically occupying 1/4 of their position.

electron density, identified with the C atoms. Refinement of the occupancy of this position showed that the C atoms statistically occupy 1/4 of it; there are four C atoms per unit cell of phase I, while in tsaregorodtsevite there were twice as many. There is no N atom at the (0 0 0) position. Upon subsequent annealing up to 970°C, the nature of the distribution of Si and Al over the tetrahedral positions changes: the two independent Si and (Si, Al) positions merge into one,  $12(d)$ , ( $1/4 1/2 0$ ), while the symmetry increases from tetragonal (space group  $I422$ ) to cubic (space group  $I432$ ). The composition of the framework is described by the formula  $[(\text{Si}_{0.833}\text{Al}_{0.167}\text{O}_2)]_2 \cdot \text{A}$

TABLE I. Some Crystallographic Characteristics of Tsaregorodtsevite and Its Annealing Products

Characteristics	Tsaregorodtsevite	Phase I, $T_{\text{ann}} = 870^\circ\text{C}$	Phase II, $T_{\text{ann}} = 970^\circ\text{C}$
Syngony	Rhombic	Tetragonal	Cubic
Unit cell parameters			
$a$	8.984(3)	8.908(1)	8.817(3)
$b$	8.937(2)		
$c$	8.927(2)	8.925(1)	
Unit cell volume, $\text{\AA}^3$	716.8(5)	708.2(1)	685.5(4)
Space group	$I222$	$I422$	$I432$
Number of formula units $z$	2	2	6
Number of independent nonzero ( $I = 1.96\sigma_f$ ) reflections	516	408	39
$\max \sin\theta / \lambda, \text{\AA}^{-1}$	0.703	0.702	
$R_{\text{hkl}}$ (aniso)	0.047	0.044	0.047
$R_w$	0.048	0.043	0.041
Composition of Si-Al-O framework	$[\text{Si}_2(\text{Si}_{0.5}\text{Al}_{0.5})\text{O}_6]_2^{-0.5}$	$[\text{Si}_2(\text{Si}_{0.5}\text{Al}_{0.5})\text{O}_6]_2^{-0.5}$	$[(\text{Si}_{0.833}\text{Al}_{0.167})\text{O}_2]_2^{-0.17}$
Density of framework $d_f, \text{\AA}^3$ (Ref. 5)	16.74	16.94	17.51
Volume per oxygen atom, $V_o, \text{\AA}^3$	29.87	29.51	25.77

TABLE III. Interatomic Distances (Å) and Bond Angles (degrees)

Tsaregorodtsevitse		(Si <sub>0.5</sub> Al <sub>0.5</sub> )-tetrahedron
Si <sub>1</sub> -tetrahedron		
Si1-O1	1.596(4) × 2	(Si, Al)-O1 1.633(4) × 2
O3	1.603(5) × 2	O2 1.627(5) × 2
Average	1.600	1.630
O1-Si1-O1	111.0(8)	O1-(Si, Al)-O1 110.3(8)
O1-Si1-O3	107.9(7) × 2	O1-(Si, Al)-O2 110.3(7) × 2
O1-Si1-O3	110.1(7) × 2	O1-(Si, Al)-O2 108.1(7) × 2
O3-Si1-O3	110.0(6)	O2-(Si, Al)-O2 109.8(6)
Average	109.5	109.5
Framework angle		
Si1-O1-(Si, Al)	159.3(8)	
Si2-O2-(Si, Al)	159.9(8)	
Si1-O3-Si2	195.5(8)	
Average	159.7	
Phase I		
(Si <sub>0.5</sub> Al <sub>0.5</sub> )-tetrahedron		Framework angle
(Si, Al)-O2	1.626(3) × 4	Si-O1-Si 160.3(2)
		Si-O2-(Si, Al) 158.5(4)
		159.4
O2-(Si, Al)-O 2	110.5(3) × 2	
O2-(Si, Al)-O 2	103.6(3) × 2	
O2-(Si, Al)-O 2	114.5(3) × 2	
		109.5
Phase II		
(Si, Al)-tetrahedron		
(Si, Al)-O	1.577(4) × 4	
O-(Si, Al)-O	107.5(2) × 2	
O-(Si, Al)-O	110.5(2) × 4	
Average	109.5	
Framework angle		
(Si, Al)-O-(Si, Al)	162.5(3)	

decrease in the (Si, Al)-O distances down to 1.577 Å led to a significant decrease in the volume of the unit cell of phase II ( $V = 685.4 \text{ \AA}^3$ ). The overall decrease in the unit cell volumes of tsaregorodtsevitse upon heating up to 970°C was 31.3 Å<sup>3</sup>, while the decrease in the specific volume of the oxygen atoms in the framework  $V_O$  was 4.10 Å<sup>3</sup>.

Thus during calcination at 870°C, we can assume degradation of the TMA cations and formation of their high-temperature amorphous densification products, containing C atoms, including elemental carbon. Further calcination at 970°C leads to full degradation of these products, and the negative change on the (Si, Al, O) framework most likely is compensated by the H<sup>+</sup> protons located in the channels. Removal of the fillers from the channels is probably a major reason for contraction of the unit cell volume in the samples calcined at 970°C.

The obvious structural changes in tsaregorodtsevitse noted with an increase in temperature support the assumption that its tetrahedral framework has relatively low stability, due to the presence of extremely large TMA cations in the channels of its structure. Such a reduction in thermal stability of the structure with an increase in the sizes of the filler in its channels has been recently noted<sup>7</sup> for the example of natrolite, in which substitution of Cs for Na reduces the temperature of the

$\alpha$ -metanatroilite- $\beta$ -metanatroilite phase transition from  $\approx 550^\circ\text{C}$  to  $\approx 160^\circ\text{C}$ .

We thank Professor N. I. Leonyuk for making it possible to anneal a single crystal of tsaregorodtsevitse in the crystal growing laboratory of the crystallography and crystal chemistry division of the geology department at Moscow State University.

<sup>1</sup>L. A. Pautov, V. Yu. Karpenko, E. V. Sokolova, and K. I. Ignatenko, *Zap. VMO*, No. 1 (1993).

<sup>2</sup>E. V. Sokolova, V. B. Rybakov, and L. A. Pautov, *Dokl. Akad. Nauk SSSR* 317, 884 (1991) [*Sov. Phys. Dokl.* 36, 267 (1991)].

<sup>3</sup>Yu. F. Shepelev, "Crystal chemistry of silicates with complex cations and the structural aspects of physicochemical processes in zeolites," *Author's Abstract, Doctoral Dissertation*, Leningrad (1990).

<sup>4</sup>A. Kawahara and S. Kohara, *Abstracts*, Twenty-Ninth IGC Kyoto (1992), Vol. 3/3, p. 696.

<sup>5</sup>F. Liebau, *Structural Chemistry of Silicates* [Russian translation], Mir, Moscow (1988).

<sup>6</sup>I. A. Belitsky, B. A. Fursenko, S. P. Gabuda, et al., *Phys. Chem. Miner.* 18, 497 (1992).

Translated by Cathy Flick